Intracellular Calibration of a pH-sensitive Dye in Isolated, Perfused Salamander Proximal Tubules

J. RICHARD CHAILLET and WALTER F. BORON

From the Department of Physiology, Yale University School of Medicine, New Haven, Connecticut 06510

ABSTRACT We evaluated the dye 4′,5′-dimethyl-5- (and -6-) carboxyfluorescein (Me_2CF) for determining the intracellular pH (pH_i) of isolated, perfused proximal tubules of the salamander. The intracellular absorbance spectrum, corrected for the intrinsic absorbance of the tubule, was obtained once per second. The dye was incorporated into tubule cells by exposing them to the membrane-permeable precursor 4′,5′-dimethyl-5- (and -6-) carboxyfluorescein diacetate. The introduction of the dye had no significant effect on either pH_i or cell voltage transients. Compared with dye contained in a cuvette, intracellular dye had a peak absorbance that was red-shifted by ~5 nm, and an apparent pK that was increased by ~0.3. These differences precluded an accurate calculation of pH_i by the comparison of intracellular spectra with in vitro calibration spectra. However, when Me_2CF was calibrated intracellularly, using the K-H exchanger nigericin to equalize external pH and pH_i, the dye-derived, steady state pH_i was within ~0.1 of the value obtained with pH-sensitive microelectrodes. Furthermore, when pH_i was simultaneously measured with dye and microelectrodes during rapid pH_i transients, the pH_i time courses measured by the two methods were very similar. We conclude that the intracellular absorbance spectrum of Me_2CF can be used to measure steady state pH_i and rapid pH_i transients reliably, provided the dye is calibrated intracellularly.

INTRODUCTION

The measurement of intracellular pH (pH_i) is important not only for predicting the behavior of pH-sensitive processes, but also for studying metabolic and transport functions that affect pH_i. The problem of measuring pH_i in renal tubule cells is of special interest for understanding the mechanisms of renal acid-base transport at the cellular level. The equilibrium distribution of the weak acid 5,5-dimethyloxazolidine-2,4-dione (DMO) (Struyvenberg et al., 1968; Kleinman et al., 1980; Bichara et al., 1980) and ^{31}P nuclear magnetic resonance spectros-

Address reprint requests to Dr. Walter F. Boron, Dept. of Physiology, Yale University School of Medicine, 333 Cedar St., New Haven, CT 06510. Dr. Chaillet's present address is Dept. of Internal Medicine, Washington University School of Medicine, St. Louis, MO 63110.

J. GEN. PHYSIOL. © The Rockefeller University Press · 0022-1295/85/12/0765/30$1.00

Volume 86 December 1985 765–794

copy (Balaban, 1982; Sehr et al., 1979) have been used to measure steady state values of pH_i in suspensions of kidney tubules. Although these methods are capable of accurately measuring pH_i, they cannot follow rapid pH_i changes in a single tubule. On the other hand, recessed-tip microelectrodes (R. C. Thomas, 1974) have been used to follow rapid pH_i changes in the isolated, perfused proximal tubule of the tiger salamander, *Ambystoma tigrinum* (Boron and Boulpaep, 1983*a*, *b*). Recently, a highly selective, pH-sensitive liquid membrane microelectrode (Ammann et al., 1981) has been used in a study of proton transport in the *Necturus* gallbladder (Baxendale and Armstrong, 1983), and in pH_i measurements in the rabbit proximal tubule (Sasaki et al., 1984). Although microelectrodes have proven very reliable in relatively large amphibian epithelial cells, there are two classes of problems that relate to the application of ion-sensitive microelectrodes to the much smaller cells of mammalian epithelia. First, given the requirement for a small electrode tip size, there are theoretical limitations to the response time of the recessed-tip microelectrode, and to the sensitivity, selectivity, and possibly the response time of the liquid membrane microelectrode. Second, there are practical difficulties in regularly obtaining impalements that are sufficiently long-lasting to monitor entire pH_i transients. By contrast, pH-sensitive dyes offer distinct theoretical and practical advantages, including a short response time, ease of use, and applicability to a single cell or small groups of cells. Furthermore, dyes have been applied successfully to the measurement of pH_i in cultured mammalian cells (J. A. Thomas et al., 1979; Moolenar et al., 1983; Vigne et al., 1982; Rothenberg et al., 1983).

In the present study, we examined the feasibility of using the absorbance spectrum of a dye to accurately measure pH_i and rapid changes in pH_i in isolated, perfused proximal tubules of the tiger salamander. We incorporated the pH-sensitive dye 4′,5′-dimethyl-5- (and -6-) carboxyfluorescein (Me_2CF) into cells of the tubule. Rapid time resolution was achieved by recording the intensity spectrum of the transmitted light on a 1,024-element photodiode array. We found that there are significant differences between the in vivo and the in vitro spectra of the dye. However, when the intracellular dye is properly calibrated, the dye-derived pH_i values are very similar to those measured with pH-sensitive microelectrodes. Moreover, during rapid pH_i transients, the dye-derived pH_i closely follows the pH_i measured simultaneously with a liquid membrane microelectrode. Finally, the dye has no discernible effect on steady state pH_i or on induced changes in pH_i and membrane potential.

METHODS

Biological Preparation

Isolated segments of the early proximal tubule (~100 μm diam) from freshly killed tiger salamanders (*Ambystoma tigrinum*) were perfused at room temperature in a manner identical to that described by Boron and Boulpaep (1983*a*). The isolated, perfused tubule apparatus was similar to that originally described by Burg and colleagues (1966). The length of tubule between the holding pipettes was reduced to 200–400 μm in order to minimize movement of the tubule in the optical path.

Solutions

The compositions of the Ringer solutions are given in Table I. In experiments in which the solutions were nominally bicarbonate-free, the standard Ringer was buffered with 13.4 mM HEPES to pH 7.5 (solution 1), whereas in experiments with bicarbonate-containing solutions, the standard Ringer was buffered to pH 7.5 with 10 mM bicarbonate and 1.5% CO_2 (solution 6). Nigericin (obtained from Calbiochem-Behring Corp., La Jolla, CA) was sometimes added to solution 5 as a stock solution (10 mM in ethanol) to a final nigericin concentration of 10 μM. 4′,5′-Dimethyl-5- (and -6-) carboxyfluorescein (Me_2CF)

TABLE I

Compositions of Solutions

Component	(1) Standard HEPES	(2) NH_4^+ HEPES	(3) pH 6.8 HEPES	(4) 0-Na^+ HEPES	(5) 0-Na^+, high-K^+ HEPES	(6) Standard HCO_3^-	(7) pH 6.8 HCO_3^-
Na^+	97.65	77.65	93.5	0.05	0.05	100.95	100.8
K^+	2.5	2.5	2.5	2.5	75.0	2.5	2.5
NH_4^+	0	20.0	0	0	0	0	0
$NMDG^+$	0	0	0	97.1	24.6	0	0
Mg^{2+}	1.0	1.0	1.0	1.0	1.0	1.0	1.0
Ca^{2+}	1.8	1.8	1.8	1.8	1.8	1.8	1.8
$Lysine^+$	0.2	0.2	0.2	0.2	0.2	0.2	0.2
meq (+)	105.95	105.95	101.8	105.45	105.45	109.25	109.1
Cl^-	94.7	94.7	94.7	94.2	94.2	94.7	102.7
HCO_3^-	0	0	0	0	0	10.0	2.0
$H_2PO_4^-$	0.1	0.1	0.25	0.1	0.1	0.1	0.25
$HPO_4^=$	0.4	0.4	0.25	0.4	0.4	0.4	0.25
$Lactate^-$	3.6	3.6	3.6	3.6	3.6	3.6	3.6
Glu^-	0.05	0.05	0.05	0.05	0.05	0.05	0.05
$HEPES^-$	6.7	6.7	2.7	6.7	6.7	0	0
meq (−)	105.95	105.95	101.8	105.45	105.45	109.25	109.1
Glucose	2.2	2.2	2.2	2.2	2.2	2.2	2.2
Gln	0.5	0.5	0.5	0.5	0.5	0.5	0.5
Ala	0.5	0.5	0.5	0.5	0.5	0.5	0.5
HEPES	6.7	6.7	10.7	6.7	6.7	0	0
pH	7.5	7.5	6.8	7.5	7.5	7.5	6.8
CO_2(%)	0	0	0	0	0	1.5	1.5
O_2(%)	20	20	20	20	20	98.5	98.5

All compositions are given in millimolar unless otherwise noted.

and 4′,5′-dimethyl-5- (and -6-) carboxyfluorescein diacetate (Me_2CFAc_2) were obtained from Molecular Probes, Inc., Junction City, OR. The Me_2CFAc_2 was sometimes added to solution 3 from a stock solution (100 mM in dimethyl sulfoxide) to a final concentration of 100 μM. *N*-Methyl-D-glucamine (NMDG) and HEPES were obtained from Sigma Chemical Co., St. Louis, MO.

Chamber

The chamber not only accommodated the pipettes of the isolated perfused tubule apparatus, but also permitted simultaneous microelectrode and optical measurements on

the same perfused tubule. The bottom of the chamber was a standard glass coverslip (thickness, 0.17 mm). The time constant for changing bath solutions, determined by measuring the time course of the bath pH after a change to a solution of different pH, was ~2 s.

Electrode Measurements

Liquid membrane microelectrodes were used to measure intracellular pH. Omega Dot borosilicate glass capillaries (1 mm o.d. × 0.5 mm i.d.; Frederick Haer & Co., Brunswick, ME) were pulled on a Brown and Flaming electrode puller (Sutter Instruments, San Francisco, CA), and had a resistance of ~10 MΩ when filled with 3 M KCl. The tips were backfilled with the pH-sensitive cocktail of Ammann et al. (1981) (obtained from Fluka Chemical Corp., Hauppauge, NY). The remainder of the shaft was backfilled with the phosphate-buffered solution of Ammann et al. (1981). The voltage-recording microelectrode was backfilled with 3 M KCl and had a resistance of ~20 MΩ. Different cells of the isolated tubule were simultaneously impaled with the voltage- and pH-sensitive electrodes. The impaled cells were on opposite sides of the 25-μm spot of incident light (see below), at least 100 μm apart. Therefore, the optical and electrical measurements were made on different cells.

A calomel electrode was used as a bath reference electrode and was placed in the bath drain line ~1 cm from the center of the chamber. The bath was grounded with a 90% Pt/10% Ir wire. The pH-sensitive and calomel electrodes were each connected to one of the dual inputs of an electrometer with 10^{15} Ω input impedance (model FD223, W-P Instruments, Inc., New Haven, CT). The voltage-sensitive electrode was connected to the input of a 10^{11}-Ω input impedance electrometer (model 750, W-P Instruments, Inc.). The signal from the calomel electrode was electronically subtracted from the voltage-sensitive electrode signal to obtain the basolateral membrane potential (V_b). The signal from the voltage electrode was subtracted from the pH electrode voltage to obtain the voltage owing to pH_i (V_{pH}). V_b and V_{pH} were recorded on a stripchart recorder and were also sampled by an analog-to-digital converter of an LSI 11/23–based computer (Digital Equipment Corp., Maynard, MA).

Optics

The central component of our optical system was a modified inverted microscope (Diavert, E. Leitz, Inc., Rockleigh, NJ), which was placed on a vibration-isolation table (model RS8, Newport Research Corp., Fountain Valley, CA). The aforementioned chamber was positioned on the stage of the microscope. The isolated, perfused tubule rested on the coverslip that formed the bottom of the chamber. A second glass coverslip was fixed ~1 mm above the tubule, thereby sandwiching the tubule and ~1 mm of solution between the two coverslips.

Fig. 1 illustrates the incident light path from the light source to the tubule, and the transmitted light path from the tubule to the photodiode array used to measure the transmitted intensity spectrum. The light source was a 12-V, 100-W quartz tungsten-halogen lamp (Osram 64625, Handsel Scientific, Freehold, NJ). We reduced sporadic air currents, which cause gross fluctuations in light intensity, by placing the bulb in a light- and air-tight, water-cooled housing. The optics were set up for Köhler illumination. Between the collecting lens and the field aperture were heat filters, a series of compensating filters, a beam-splitting cube, and a field-diaphragm/shutter assembly. Two heat filters (KG-3, Schott Glass Technologies, Inc., Duryea, PA) were used to limit infrared radiation. Four compensating filters (custom-made interference filters obtained from Omega Optical, Inc., Brattleboro, VT) were used not only to eliminate light of wavelengths

shorter than 400 nm, but also to equalize (within a factor of 2) light intensities between 400 and 800 nm. A 1-cm beam-splitting cube (Melles-Griot, Irvine, CA) diverted 50% of the light to a UV-100B photodiode (EG&G, Electro-Optics Division, Salem, MA), the output of which was used in a feedback circuit to control the power supply (model ATE 15-15M, Kepco, Inc., Flushing, NY), and thereby stabilize the light intensity. The field aperture consisted of two 800-μm-diam pinholes (center-to-center separation, ~3 mm), each with its own computer-controlled shutter.

The condenser was a Leitz L32 objective with a working distance of 6.6 mm, and a maximal numerical aperture (NA) of 0.4. However, in order to minimize spherical

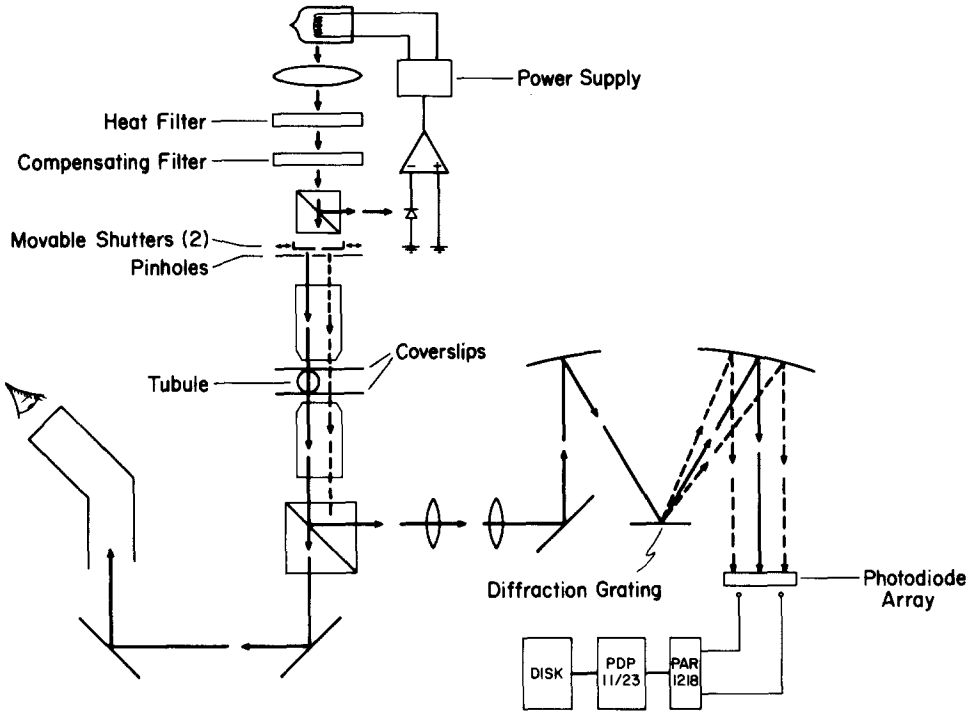

FIGURE 1. Schematic diagram of the optical system. The isolated, perfused tubule is located between the two coverslips, on the stage of an inverted microscope. See text for details.

aberrations, we stopped down the condenser aperture to an NA of ~0.1. The condenser focused the pinholes in the plane of the tubule, one on the tubule and one off the tubule. Because the magnification of the condenser was 32, the pinhole images were 25 μm in diameter and were separated by 100 μm.

The transmitted light was collected by a 10×, 0.4-NA objective (Wild Heerbrugg Instruments, Inc., Farmingdale, NY). The image of the tubule was then focused onto the entrance slit of a polychromator (model HR-320, Instruments S.A., Inc., Metuchen, NJ) using a field/relay-lens combination. This arrangement of the lenses reduced the NA of the collected transmitted light from 0.4 at the objective to 0.1 at the entrance slit, and also magnified the 25-μm-diam image approximately fourfold to ~100 μm.

The light entering the polychromator was collimated and projected onto a diffraction grating (147 g/mm). One of the first-order bands of the diffracted light, between wavelengths of 350 and 850 nm, was then focused onto a 1,024-element photodiode array detector (model 1412, EG&G Princeton Applied Research Corp., Princeton, NJ). The magnification from the entrance slit to the photodiode array was unity. For an image size of 100 μm at the entrance slit and a wavelength dispersion of 0.5 nm per photodiode (each 25 μm wide), the final wavelength resolution was ~2 nm. The wavelength calibration of the photodiode array was obtained with an interference filter having numerous known 1-nm bandwidth peaks (Omega Optical, Inc.).

Data Acquisition

The photodiode array was interfaced with a detector-controller (model 1218, EG&G Princeton Applied Research Corp.), which held the temperature of the array at −20°C. The detector-controller also programmed the array for sampling intensity spectra. Because the wavelength resolution of the optical system was ~2 nm, we summed the analog signals from every two contiguous photodiodes, and thus obtained a 512-point spectrum. In order to maximize the signal for analog-to-digital conversion, we also increased the signal-integration time of each photodiode from the minimum period of 16 to ~800 μs. Thus, the minimum time required for a complete scan of 1,024 photodiodes was ~820 ms. Finally, the detector-controller performed a 14-bit analog-to-digital conversion. The digitized information was passed to a direct-memory-access parallel interface (DRV-11B, Digital Equipment Corp.). The use of the photodiode array for spectroscopy is described by Talmi and Simpson (1980).

Determination of Absorbance Spectra

The absorbance measured in our experiments has two components: the true absorbance of the dyed tubule, and an apparent absorbance caused by uncollected scattered light. The absorbance (A) at a given wavelength is calculated from the equation:

$$A = \log[(I_o - I_{dark})/(I - I_{dark})],$$

where I_o is the light intensity in the absence of a tubule, I_{dark} is the measured intensity in the absence of incident light, and I is the intensity in the presence of a tubule.

Cuvette Calibration

In vitro absorbance spectra of Me_2CF were obtained with the auxiliary port of the same polychromator used in the isolated, perfused tubule experiments. The cuvette was placed on an optical bench, adjacent to the polychromator, mounted on the vibration-isolation table.

RESULTS

pH Dependence of Dye In Vitro

Fig. 2 illustrates a series of absorbance spectra at pH values ranging from 5.74 to 7.71, obtained in a 1-cm cuvette, at a dye concentration of 10 μM. Regardless of the pH, the original spectra had an absorbance of 0.19 at 470 nm, the isosbestic wavelength. From this absorbance, we calculated a molar extinction coefficient (ϵ_{470}) of 1.90×10^4 M^{-1} cm^{-1}. For the sake of simplicity, we scaled the original spectra to an absorbance of unity at 470 nm. At high pH, the absorbance is maximal at 505 nm. The ratio of the peak absorbance to the

absorbance at the isosbestic wavelength is plotted in the inset of Fig. 2 as a function of pH. The curve drawn through the points is the result of a nonlinear least-squares curve fit to a standard pH titration curve. The best-fit pK_a value is 6.90 ± 0.01. The 10 μM dye concentration used in these cuvette calibrations was substantially lower than the 2–4-mM concentrations used in our intracellular experiments (see below). We therefore obtained in vitro dye calibration spectra similar to those of Fig. 2 at dye concentrations of 100 μM to 6 mM (see Table II). [Me_2CF] had little effect on the upper and lower asymptotes of the titration curve between 10 μM and 6 mM, and no significant effect on pK_a between 10

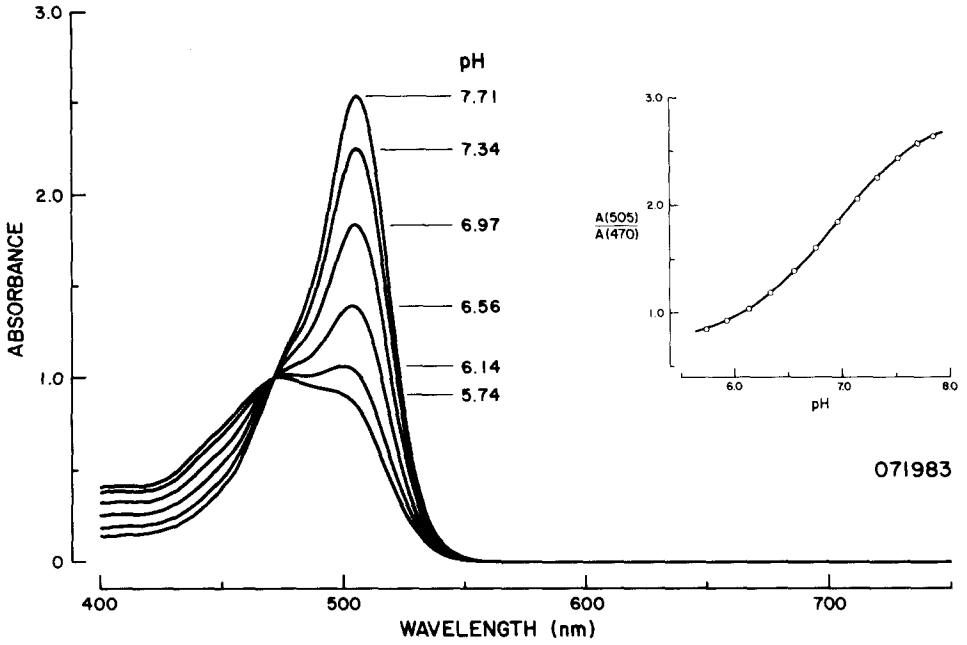

FIGURE 2. pH dependence of the in vitro absorbance spectra of Me_2CF. Of the 12 spectra obtained, 6 are shown. 10 μM dye was placed in a 1-cm cuvette. The solutions contained 100 mM K^+, and were buffered with 40 mM PIPES. The inset is the ratio of the peak absorbance (at 505 nm) to the absorbance at the isosbestic wavelength (470 nm), plotted as a function of pH.

and 100 μM. However, as [Me_2CF] was raised from 100 μM to 6 mM, the pK_a increased from 6.90 to 7.12. A similar effect of dye concentration on pK_a has been described by Babcock (1983) for carboxyfluorescein. The effect of dye concentration on the shape of the absorbance spectrum is discussed on p. 779.

Me_2CF does not measurably absorb at wavelengths of >560 nm. Furthermore, its absorbance is insensitive to 2 mM Ca^{2+} or Mg^{2+}. As discussed in more detail below, the peak absorbance and the isosbestic wavelength of intracellular dye are generally red-shifted (i.e., to higher wavelengths) by 3–6 nm compared with the in vitro dye.

Loading Cells with Dye

We incorporated Me_2CF into cells of an isolated, perfused tubule by perfusing the tubule with pH 6.8 HEPES Ringer (solution 3) containing 100 μM of the colorless diacetate ester of Me_2CF, Me_2CFAc_2. This diacetate precursor enters the cells, where it is hydrolyzed by acetylesterases (Rotman and Papermaster, 1966; J. A. Thomas et al., 1979), yielding Me_2CF (see Fig. 3*A*). The time course of the incorporation of intracellular dye[1] [as indicated by $A(470)$], during an exposure of the tubule to Me_2CFAc_2, is illustrated in Fig. 3*B*. Permeable precursors of ion-sensitive dyes have been similarly employed with other fluorescein derivatives (J. A. Thomas et al., 1979; Rink et al., 1982) and with the Ca-sensitive indicator quin 2 (Tsien, 1981).

Obtaining Intracellular Dye-specific Spectra

Fig. 4 illustrates the effect of lowering the basolateral HCO_3^- concentration ($[HCO_3^-]_b$) on the peak absorbance of intracellular dye (511 nm in this experiment). The initial value of $A(511)$ in this experiment was subtracted from all

TABLE II

*Summary of Cuvette pH Titration Data for Me_2CF**

[Me_2CF]	pK_a	Lower asymptote	Upper asymptote
(1) 10 μM	6.90±0.01	0.71±0.01	2.83±0.01
(2) 100 μM	6.90±0.01	0.71±0.01	2.73±0.01
(3) 500 μM	6.96±0.01	0.71±0.01	2.83±0.01
(4) 1 mM	6.96±0.01	0.70±0.01	2.80±0.01
(5) 3 mM	7.05±0.01	0.71±0.01	2.76±0.01
(6) 6 mM	7.12±0.01	0.72±0.01	2.81±0.01

* Absorbance ratio data were fitted to a standard titration curve by a nonlinear least-squares method. Fitted values are listed ± standard deviation.

data points in Fig. 4. Reducing $[HCO_3^-]_b$ from 10 to 2 mM (solutions 6 to 7) at constant pCO_2 (i.e., lowering pH_b from 7.5 to 6.8) is known to cause a rapid and reversible fall of pH_i in the salamander proximal tubule (Boron and Boulpaep, 1983*b*). Fig. 4*A* shows that, even in the absence of dye, this reduction of $[HCO_3^-]_b$ and pH_b caused changes in $A(511)$. The reduction of $[HCO_3^-]_b$ caused $A(511)$ to rapidly fall slightly below the initial value indicated by point 1, and then to slowly rise to a level indicated by point 2. Subsequently returning $[HCO_3^-]_b$ and pH_b to normal results in opposite shifts in $A(511)$. Comparable absorbance changes are observed throughout the visible spectrum. These changes in the absorbance of the tubule cells per se (i.e., intrinsic absorbance) could be due to several factors, including changes in pH_i and cell volume. Indeed, when we induced changes in cell volume by exposing the tubule to anisotonic media, we saw comparable changes in the intrinsic absorbance. The changes probably do not, in general, represent only pH_i changes, inasmuch as intracellular

[1] As noted below, the intracellular isosbestic wavelength varies between 471 and 477 nm. Only at the isosbestic wavelength is the dye's absorbance proportional to the dye concentration and yet totally independent of pH. Nevertheless, the error made in monitoring $A(470)$ is minimal, inasmuch as the pH dependence at this wavelength is very slight.

acidification was sometimes associated with a decrease in intrinsic absorbance changes.

In Fig. 4*B*, the identical change in $[HCO_3^-]_b$ and pH_b was made after the incorporation of Me_2CF in the same tubule. The much larger fall of $A(511)$ was produced by the sum of the changes in dye-specific and intrinsic absorbance. The dye-specific absorbance, needed to calculate pH_i, could in theory be obtained

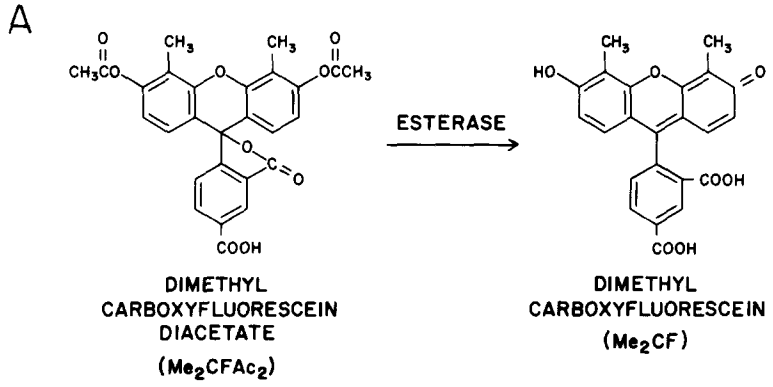

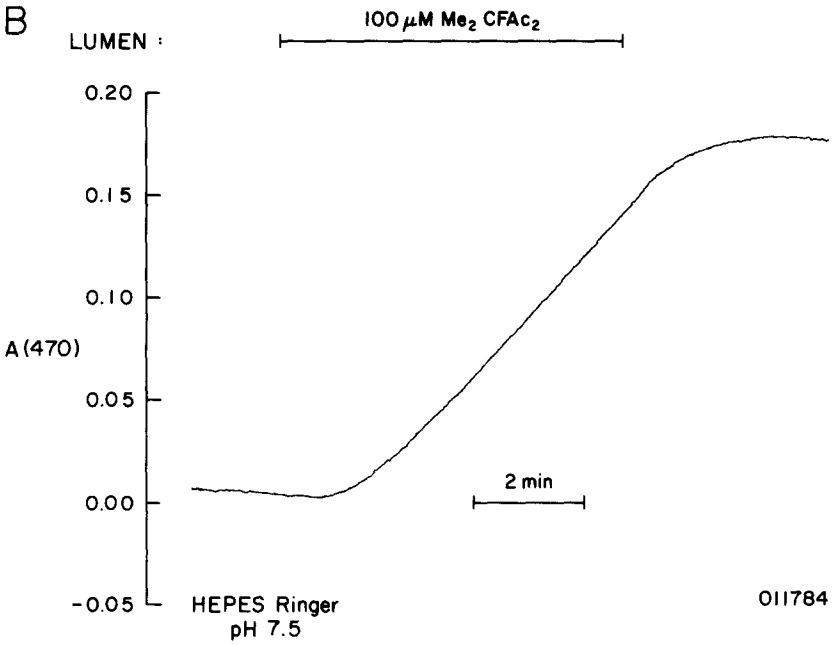

FIGURE 3. (*A*) Hydrolysis of Me_2CFAc_2 to Me_2CF. (*B*) Time course of absorbance at 470 nm upon introduction of 100 μM Me_2CFAc_2 to the lumen. $A(470)$ is approximately proportional[1] to $[Me_2CF]_i$. All solutions were HCO_3^--free and were buffered with HEPES. The Me_2CFAc_2-containing solution had a pH of 6.8 (solution 3), and the other solution had a pH of 7.5 (solution 1).

by subtracting the intrinsic absorbance change (Fig. 4*A*) from the total absorbance change (Fig. 4*B*), as illustrated by the "subtracted" curve in Fig. 4*D*. This simple subtraction method of obtaining dye-specific absorbance is valid only if the change of intrinsic absorbance in Fig. 4*B* is the same as that in Fig. 4*A*.

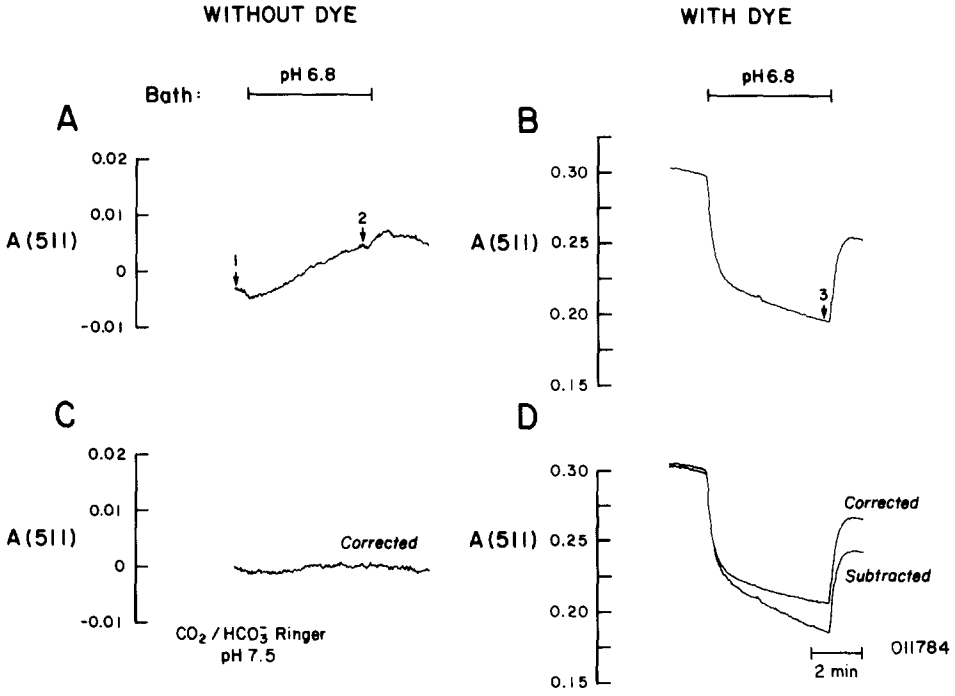

FIGURE 4. Time course of peak absorbance (511 nm) during a reduction of bath pH in HCO_3^- Ringer, before and after incorporation of dye. All four panels are data from the same tubule. The initial tubule absorbance at 511 nm has been subtracted from all records. (*A*) Unmodified *A*(511) time course in an undyed tubule. The bath pH was reduced from 7.5 (10 mM HCO_3^-) to 6.8 (2 mM HCO_3^-) at a constant pCO_2 (solutions 6 and 7, respectively). The numeral 1 indicates a time just before the introduction of the pH 6.8 solution, and the 2 indicates a time just before the return to the pH 7.5 solutions. (*B*) Unmodified *A*(511) time course after incorporation of dye. The numeral 3 indicates a time just before the return from pH 6.8 to pH 7.5 Ringer. (*C*) Corrected *A*(511) time course in the absence of dye. This tracing was derived from that of *A* by applying the correction described in the text. (*D*) Subtracted and corrected *A*(511) time courses in the presence of dye. The subtracted tracing is the difference between the traces in *B* and *A*. The corrected tracing was derived from the subtracted one by applying the same correction as that used in *C*.

Although we cannot directly compare the intrinsic absorbance changes at 511 nm in *A* and *B*, because the intrinsic absorbance change of *B* is masked by dye absorbance, we can compare them at wavelengths at which the dye does not absorb (i.e., >560 nm). Indeed, we found that the absorbance changes at 600

nm are not the same during the low-$[HCO_3^-]_b$ periods of *A* and *B* (not shown). Thus, assuming that a similar discrepancy exists at 511 nm, we can conclude that, without a further correction, the simple subtraction procedure does not yield the true absorbance of intracellular dye.

A better approach for obtaining a dye-specific absorbance might be to use the absorbance changes at wavelengths where the dye does not absorb to "correct" the aforementioned simple subtraction for intrinsic absorbance changes at wavelengths where the dye does absorb. As described in detail below, we have developed such a method for correcting spectra for intrinsic absorbance changes. Ideally, this correction should eliminate the $[HCO_3^-]_b$-dependent intrinsic absorbance changes in the absence of dye. Fig. 4*C* shows that this correction does largely eliminate intrinsic absorbance changes in the dye-free tubule of Fig. 4*A*. Therefore, it is reasonable to suppose that this correction can also be accurately applied to a dyed tubule. The curve labeled "Corrected" in Fig. 4*D* is the result of applying this correction to the *A*(511) time course in the dye-containing tubule of Fig. 4*B*, and thus approximates the time course of dye-specific absorbance.

The absorbance spectra of Fig. 5 are taken from the experiment of Fig. 4. In Fig. 5*A*, the spectrum labeled "(1) pH 7.5" is taken at the time indicated by the numeral 1 in Fig. 4*A*, and the spectrum labeled "(2) pH 6.8" is taken at the time indicated by the numeral 2. Because the tubule is as yet unexposed to Me_2CFAc_2, these are intrinsic absorbance spectra. The spectrum labeled "Subtracted (2 − 1)" (Fig. 5*C*) represents the change in the intrinsic absorbance spectrum caused by a reduction of $[HCO_3^-]_b$. This change of intrinsic absorbance is small and is in the same direction at all wavelengths. We would like to determine the correction that, when applied to the subtracted spectrum, would reduce the absorbance discrepancy to zero at all wavelengths. Using a least-squares method, we fitted the subtracted spectrum of Fig. 5*C* to a straight line between 600 and 750 nm, extrapolated the straight line to 400 nm, and took the difference between the subtracted spectrum and this extrapolated line. The result is the corrected spectrum of Fig. 5*E*, which deviates negligibly from zero.

Fig. 5, *B*, *D*, and *F*, illustrates the steps used in applying a comparable correction to the same tubule after incorporation of the dye. The spectrum labeled "(3) pH 6.8" is taken at the time indicated by the numeral 3 in Fig. 4*B*, and the one labeled "(1) pH 7.5" is again taken at the time indicated by the 1 in Fig. 4*A*. The spectrum labeled "Subtracted (3 − 1)" in Fig. 5*D* is the difference of these two spectra, and is nonzero in the region where the dye does not absorb. When this nonzero absorbance between 600 and 750 nm is fitted to a straight line, and this line is extrapolated to 400 nm and subtracted from the spectrum of Fig. 5*D*, the result is the corrected spectrum of Fig. 5*F*. This approximates the absorbance spectrum of intracellular dye.

Calibration of Intracellular Dye

PEAK AND ISOSBESTIC WAVELENGTHS OF INTRACELLULAR DYE The absorbance peak of the in vivo dye was always red-shifted by 3–6 nm compared with the in vitro dye. We have also attempted to determine whether there is a shift in the isosbestic wavelength. Our approach was to examine absorbance spectra

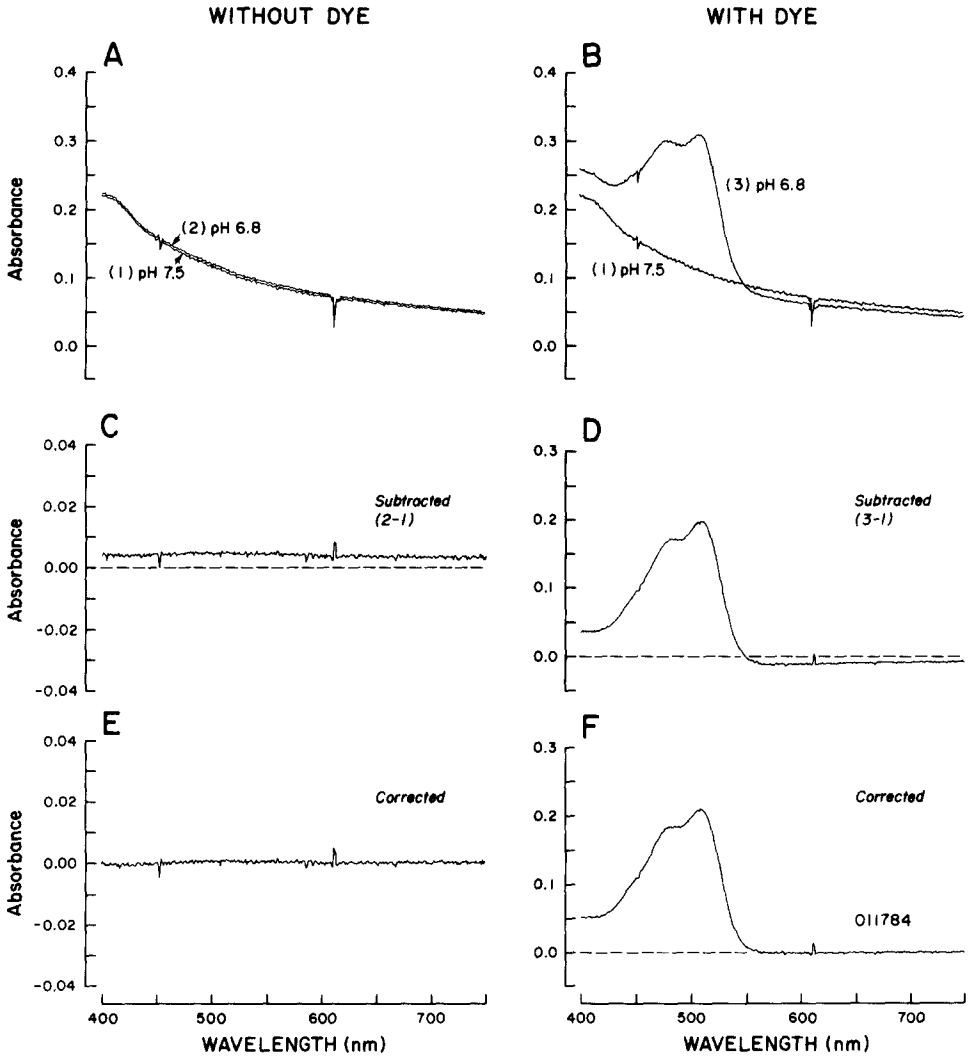

FIGURE 5. Obtaining corrected absorbance spectra in a dye-free and dye-containing tubule. The data of all six panels were taken from the same tubule as the data of Fig. 4. (*A*) Absorbance spectra of the undyed tubule, from 400 to 750 nm. The spectrum labeled "(1) pH 7.5" was taken at time 1, and that labeled "(2) pH 6.8" was taken at time 2 in Fig. 4*A*. (*B*) Absorbance spectrum of the dyed tubule. The spectrum labeled "(3) pH 6.8" was taken at time 3 in Fig. 4*B*. The spectrum labeled "(1) pH 7.5" is identical to spectrum 1 of the undyed tubule in *A*. (*C*) Result of subtracting spectrum 1 of *A* from 2 (undyed tubule). The ordinate is amplified approximately fivefold with respect to that in *A*. (*D*) Result of subtracting spectrum 1 of *B* from 3 (dyed tubule). (*E*) Corrected spectrum of undyed tubule, derived from the subtracted spectrum of *C*. (*F*) Corrected spectrum of dyed tubule, derived from the subtracted spectrum of *D*.

obtained during rapid pH_i changes, and to determine the wavelength at which no absorbance change occurred. The rapid pH_i changes were those induced by the application and removal of NH_4^+ (see discussion of Fig. 6 for an explanation). Because large pH_i changes occurred in just a few seconds, changes in $[Me_2CF]_i$ were probably negligible. We found that at pH_i values greater than ~6.7, the isosbestic wavelength of the intracellular dye was between 471 and 477 nm.

In the analysis that follows, we compute dye-derived pH_i values from the ratio A(peak)/A(470), rather than from A(peak)/A(isosbestic). The reason for not using the true isosbestic wavelength is a practical one: although we can easily measure the wavelength of peak absorbance in each experiment, it is not practical to do so for the isosbestic wavelength. Moreover, the choice of A(470) rather than of, say, A(474) in calculations of pH_i is not critical. It is the shape of the absorbance spectrum that is pH sensitive. In principle at least, pH_i (i.e., the change in spectral shape) can be determined from the ratio of absorbances at any two wavelengths. A(peak)/A(474), of course, is far more sensitive to pH changes than is, say, A(peak)/A(505). However, the reduction in sensitivity that results from choosing 470 nm instead of the true isosbestic wavelength is probably negligible. The use of A(470) introduces no error into our calculations of pH_i.

DETERMINATION OF pH_i FROM IN VITRO SPECTRA Our first approach for determining pH_i was to compare the intracellular dye-specific absorbance spectrum with a series of in vitro calibration spectra. Assuming that the ratio of the intracellular peak absorbance to A(470) is comparable to A(505)/A(470) of the in vitro spectrum, we estimated pH_i from the in vitro pH titration curve (Fig. 2, inset). In a total of 25 tubules, exposed from both the lumen and bath to pH 7.5 HEPES Ringer (solution 1), the mean initial A(peak)/A(470) was 2.09 ± 0.03. This corresponds to a pH_i of 7.18. In another study, performed under identical conditions, the pH_i of salamander proximal tubules, measured with recessed-tip, pH-sensitive electrodes, was 7.43 (Boron and Boulpaep, 1983*a*). Assuming that the pH-sensitive electrodes accurately measured pH_i, this discrepancy raises the question of whether the dye can be used to measure pH_i. We investigated three possible explanations for this discrepancy: (*a*) the dye may have reduced pH_i; (*b*) the intracellular absorbance spectrum may have been altered by the relatively high concentration of the dye necessary to perform the experiments; (*c*) the intracellular behavior of the dye may be fundamentally different from the in vitro behavior, making the application of the in vitro calibration invalid.

EFFECT OF DYE ON pH_i Fig. 6*A* illustrates the effect of dye incorporation on steady state pH_i and the recovery of pH_i from an NH_4^+-induced acid load (Boron and De Weer, 1976). pH_i was measured with a microelectrode, and the solutions were nominally HCO_3^--free. The initial pH_i was ~7.47. Between *a* and *c*, the tubule was exposed to Ringer containing 20 mM NH_4^+ (solution 2) from both the lumen and the bath. The initial, rapid rise of pH_i (*ab*) was due to the influx of the weak-base NH_3, whereas the slower fall of pH_i (*bc*) resulted from the influx of the weak-acid NH_4^+. When the external NH_4^+ was removed, there was a rapid fall of pH_i (*cd*) followed by a spontaneous, exponential recovery (*de*), having a time constant of 72 s. The *cd* fall reflects the efflux of NH_3, whereas the *de* recovery was due to Na-H exchange at the luminal and basolateral

membranes (Boron and Boulpaep, 1983*a*). During segment *ef*, the tubule was exposed to pH 6.8 HEPES Ringer (solution 3) containing 100 μM Me_2CFAc_2. The small decline of pH_i (~0.1) was due to the reduction of luminal pH and may have been augmented by the hydrolysis of the dye precursor, which generates

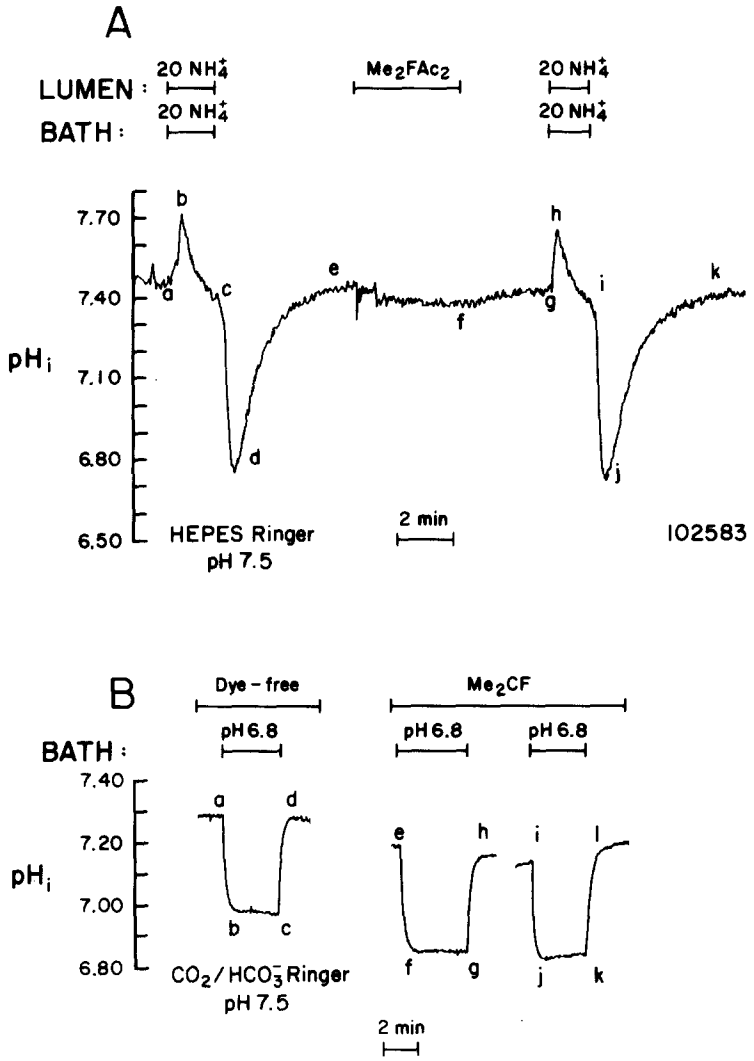

FIGURE 6. Effect of dye on pH_i transients in the absence and the presence of HCO_3^-. (*A*) NH_4^+-induced pH_i transients before and after incorporation of the dye. See text for details. (*B*) pH_i transients induced by altering basolateral [HCO_3^-]. See text for details.

acetic acid. Whatever the cause of the acidification, pH_i recovered fully after removal of the Me_2CFAc_2 (*fg*). In this experiment, the final intracellular [Me_2CF] of 2.7 mM (determined from the in vitro extinction coefficient at 470 nm) was comparable to that of other experiments. A second NH_4^+ exposure, in the

presence of intracellular dye, produced a series of pH_i changes nearly identical to those of the first. The time constant of the exponential pH_i recovery (*jk*) was 83 s, which is nearly identical to that of the *de* pH_i recovery. Furthermore, the pH_i values at points *a*, *e*, *g*, and *k* are all within 0.04 pH units of one another. Similar results were obtained in two other experiments, except that the magnitudes of the *ef* pH_i decline were somewhat larger. Thus, intracellular dye appears to have little or no effect on Na-H exchange. Furthermore, because the dye has no effect on steady state pH_i, the apparent discrepancy between dye and microelectrode estimates of pH_i cannot be explained by a toxic effect of the dye.

We also investigated the effect of intracellular dye on another transport system that can affect pH_i, the basolateral HCO_3^- transporter. In the experiment of Fig. 6*B*, we lowered $[HCO_3^-]_b$ before and after incorporation of Me_2CF, monitoring pH_i with a microelectrode. Reducing $[HCO_3^-]_b$ from 10 to 2 mM (as in the experiment of Fig. 4) caused a rapid and sustained fall of pH_i (*a–c*) because of the basolateral efflux of HCO_3^- and the likely inhibition of the basolateral Na-H exchanger (Boron and Boulpaep, 1983*b*). Returning $[HCO_3^-]_b$ to 10 mM caused a rapid recovery of pH_i (*cd*), because of HCO_3^- uptake and Na-H exchange (Boron and Boulpaep, 1983*b*). During the break in the record, the tubule was perfused for 6 min with a pH 6.8 HEPES Ringer (solution 3) containing the dye precursor. During this period, the pH-sensitive electrode fell out and was introduced into a nearby cell. This could account for the discrepancy of ~0.07 in steady state pH_i values before and after dye incorporation. In the presence of 2.0 mM intracellular dye, $[HCO_3^-]_b$ was reduced to 2 mM twice more (*e–h* and *i–l*). The time courses of the pH_i declines were well described by single exponentials, having time constants of 16 and 19 s in segments *ef* and *ij*, respectively. These are very similar to the *ab* time constant, 17 s. The extent of the pH_i changes were 0.34 in both segments *ef* and *ij*, which is very similar to the value of 0.31 obtained in the absence of dye (segment *ab*). When $[HCO_3^-]_b$ was returned to 10 mM, pH_i recovered with time constants of 17 and 14 s in segments *gh* and *kl*, respectively. These values are similar to the time constant of 12 s obtained in the absence of dye (*cd*). Similar results were obtained in two other experiments. Thus, the basolateral HCO_3^- transporter, like the Na-H exchanger, is minimally affected by Me_2CF.

EFFECT OF DYE CONCENTRATION ON THE ABSORBANCE SPECTRUM Another possible explanation for the apparent discrepancy between dye and microelectrode estimates of pH_i is that the dependence of $A(\text{peak})/A(470)$ on pH is altered by the high intracellular dye concentrations of our experiments. We tested this possibility by determining the relationship between $A(\text{peak})/A(470)$ and $[Me_2CF]$, both in vitro and in vivo. Fig. 7*A* is a plot of the in vitro $A(505)/A(470)$ vs. $[Me_2CF]$ at a fixed pH of 7.36. As can be seen, the absorbance ratio was independent of $[Me_2CF]$ at dye concentrations of <0.5 mM. For dye concentrations exceeding 0.5 mM, however, the absorbance ratio steadily declined. We found a similar effect at a fixed pH of 6.86. These results are consistent with the observations of Babcock (1983) on carboxyfluorescein.

In order to determine whether a similar effect occurs in vivo, we monitored $A(\text{peak})/A(470)$ as we increased $[Me_2CF]_i$. Throughout the experiment, pH_i was nominally clamped at 7.00 by exposing the cells to a pH 7.00 solution containing

10 μM nigericin and 75 mM K^+ (solution 5). Nigericin is a cation-hydrogen exchanger that has a high selectivity for K^+ (Pressman, 1976). If the intracellular and extracellular K^+ activities are equal, then the steady state pH_i should equal pH_o. $[K^+]_o$ in our experiments was chosen to provide an extracellular K^+ activity approximately equal to the intracellular value measured in *Ambystoma* proximal tubules (Sackin and Boulpaep, 1981), ~55 mM. This value is very similar to the values reported by others for *Necturus* proximal tubule cells (Khuri et al., 1972;

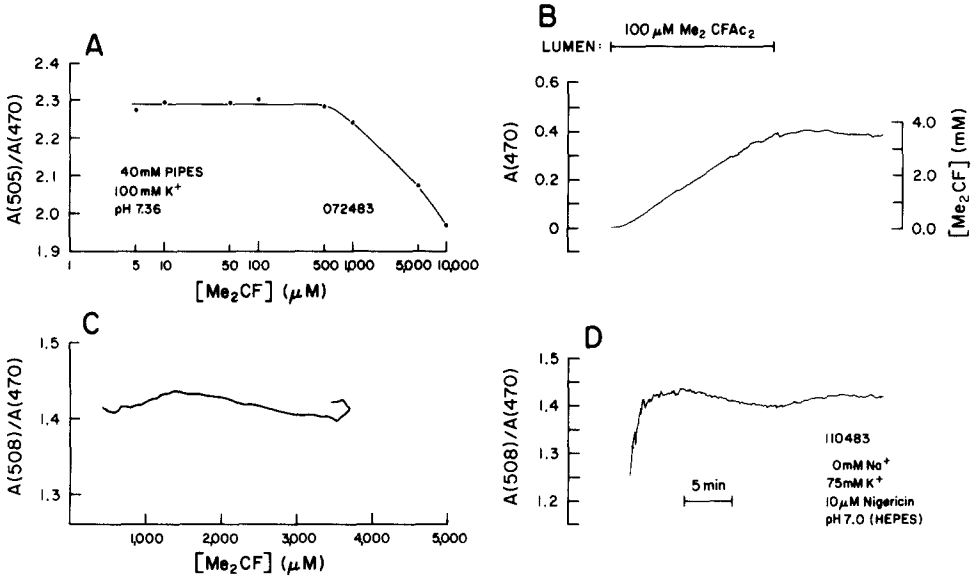

FIGURE 7. Effect of dye concentration on the in vitro and in vivo dye absorbance ratios. (*A*) In vitro dependence of $A(505)/A(470)$ on $[Me_2CF]$. The solutions contained 100 mM K^+, and were buffered to pH 7.36 with 40 mM PIPES. As $[Me_2CF]$ was increased from 5 μM to 10 mM, the cuvette path length was decreased from 1 cm to 10 μm. (*B*) Time course of $A(470)$ during introduction of Me_2CFAc_2 to the lumen only. pH_i was nominally clamped to 7.0 by exposing the tubule to a pH 7.0 Na-free solution containing 75 mM K^+ and 10 μM nigericin (solution 5). Three similar experiments were performed, one at a pH value of 7.0, and two at a pH value of 7.2. (*C*) In vivo dependence of $A(508)/A(470)$ on $[Me_2CF]$. These data are derived from those of *B*, as well as comparable data at 508 nm. (*D*) Time course of $A(508)/A(470)$ during and after introduction of Me_2CFAc_2. These data are also derived from the time course of $A(470)$ in *B*, as well as the simultaneously obtained $A(508)$ time course.

Kubota et al., 1980). We have two lines of evidence that the nigericin approach is at least approximately valid for salamander proximal tubules. The first is data suggesting that intra- and extracellular K^+ activities are approximately equal in the presence of nigericin. In four experiments, we were able to monitor cell voltage (V_m) before, during, and after an application of nigericin and 75 mM K^+. If the intra- and extracellular K^+ activities were equal, and if the cell membrane were perfectly K^+ selective, then V_m should have been 0 mV. Indeed, we found

that V_m initially had a typically negative value (i.e., −50 to −60 mV) in standard HEPES Ringer (solution 1), fell to within 10 mV of 0 upon application of nigericin/75 mM K^+ (in the pH_o range ~6 to ~8), and then partially recovered (to ~30 mV) upon removing the nigericin and returning to solution 1. The second line of evidence is data suggesting that changes in $[K^+]_o$ have only minor effects on A(peak)/A(470). We found that raising $[K^+]_o$ from 75 to 85 mM at a constant pH_o of 8.0 caused A(peak)/A(470) to increase by ~0.05 (not shown). Conversely, lowering $[K^+]_o$ to 65 mM caused the ratio to fall by ~0.03 (also not shown). Similar results were obtained when identical $[K^+]_o$ changes were made at a pH_o of 6.8 in the same tubule. Thus, our data suggest that the intra- and extracellular K^+ activities are approximately equal in the presence of nigericin, and, furthermore, that the choice of $[K^+]_o$ is not critical. Independent evidence for the validity of the nigericin/high-K^+ approach comes from J. A. Thomas et al. (1979), who have shown that 13 μM nigericin plus 130 mM K^+ approximately equalizes pH_i and pH_o in Ehrlich ascites tumor cells. The potential difficulties of the nigericin approach for clamping pH_i are treated in the Discussion.

Fig. 7*B* illustrates the increase of isosbestic wavelength absorbance as the cells incorporate Me_2CF. The ordinate was also calibrated in $[Me_2CF]_i$, assuming a path length of 58 μm and an ϵ_{470} of 1.9×10^4 M^{-1} cm^{-1} (the value obtained in the cuvette calibrations for $[Me_2CF]$ levels of 10 μM to 10 mM). $[Me_2CF]_i$ increased to a maximum of ~3.7 mM during the exposure to Me_2CFAc_2, and then slowly declined to ~3.5 mM after the precursor was removed.

Fig. 7*D* is a plot of the time course, from the same experiment, of the ratio of absorbance at the peak (i.e., 508 nm) to that at 470 nm. Early in the experiment, the individual absorbances were so low that the absorbance ratio could not be accurately calculated. The initial ratio of 1.25 was thus artifactually low. However, as $[Me_2CF]_i$ increased, A(470) and A(508) rose to levels that could be accurately measured (i.e., ~0.05), and A(508)/A(470) peaked at ~1.43. As $[Me_2CF]_i$ reached ~1.7 mM, at a time when $[Me_2CF]_i$ was increasing most rapidly, A(508)/A(570) fell to ~1.40. This slight decline is probably due to the rapid generation of acetic acid from the dye precursor. When the precursor was finally removed from the lumen, A(508)/A(470) recovered to the previous peak value of ~1.43.

The data of Fig. 7, *B* and *D*, are replotted as A(508)/A(470) vs. $[Me_2CF]_i$ in Fig. 7*C*. As $[Me_2CF]_i$ increased from ~500 to ~1,400 μM, A(508)/A(470) rose from ~1.40 to ~1.43. This small rise is probably due to the inaccuracy of the absorbance measurements at low $[Me_2CF]_i$. As $[Me_2CF]_i$ increased from ~1,400 to ~3700 μM, A(508)/A(470) declined to ~1.40, reflecting the likely pH_i decline caused by the generation of acetic acid. The final increase in A(508)/A(470) at approximately constant $[Me_2CF]_i$ (i.e., ~3,800 μM) was the result of the increase in pH_i that accompanied the washout of dye precursor. Thus, the final A(508)/A(470) at a $[Me_2CF]_i$ of ~3,800 μM (i.e., 1.43) was nearly the same as A(508)/A(470) at ~1,400 μM, which indicates that, at a stable pH_i, A(508)/A(470) is independent of intracellular dye concentration between ~1 and 4 mM. Because $[Me_2CF]_i$ in our other experiments fell within this 1–4-mM concentration range, we can disregard dye concentration as a factor influencing the calculation of pH_i.

The concentration dependence of intracellular dye contrasts sharply with that of in vitro dye (Fig. 7*A*), for which $A(505)/A(470)$ varied substantially over the 1–4-mM dye concentration range. Although we have no explanation for this discrepancy, it is possible that intracellular binding or metabolism of the dye prevents the dye-dye interaction that is the likely cause of the in vitro concentration dependence of $A(505)/A(470)$ demonstrated in Fig. 7*A*. If this is the case, then one might expect other spectral evidence of dye binding or metabolism.

PH CALIBRATION OF INTRACELLULAR SPECTRA Inasmuch as the apparent discrepancy between the dye- and microelectrode-derived pH_i values cannot be ascribed either to dye toxicity or to the concentration dependence of the dye spectrum, it is probably due to the idiosyncratic behavior of the dye within the cell. Our approach for accurately determining pH_i from an intracellular absorbance spectrum was to obtain a series of intracellular absorbance spectra at known pH_i values. Fig. 8*A* illustrates an experiment in which a tubule, previously loaded with Me_2CF, was exposed to pH 7.5 HEPES Ringer (solution 1) containing 2.5 mM K^+. Throughout this experiment, the lumen and bath solution were identical. The initial $A(511)/A(470)$ was 1.96. At this point, 10 μM nigericin was added, K^+ was raised to 75 mM, and pH_o was raised to 8.10. Because nigericin has a slight affinity for Na^+ as well as for K^+, we also removed Na^+ from all subsequent solutions. This change from normal HEPES Ringer to the pH 8.10 nigericin-containing Ringer (solution 5, adjusted to pH 8.10) caused $A(511)/A(470)$ (i.e., pH_i) to increase slowly and stabilize. Subsequent reductions of pH_o, in steps of ~0.3, led to corresponding reductions in $A(511)/A(470)$.

Fig. 8*B* is a collection of intracellular absorbance spectra obtained from the experiment of Fig. 8*A*, during times when $A(511)/A(470)$ had stabilized. In order to compare the shapes of the spectra, we normalized the spectra so that $A(470)$ was unity. Although these intracellular spectra bear a superficial resemblance to the in vitro spectra of Fig. 2, there are slight differences that become apparent when the two are directly compared. Fig. 9 is a plot of an in vitro pH 7.53 spectrum ($[Me_2CF] = 10$ μM) and the in vivo pH 7.52 spectrum of Fig. 8*B* ($[Me_2CF] = 3.6$ mM), each normalized to an $A(470)$ of unity. Compared with the in vitro spectrum, the in vivo spectrum has an $A(peak)/A(470)$ that is substantially lower, and a peak that is red-shifted by 6 nm. Neither the peak reduction nor the red shift was observed in experiments in which Me_2CF was perfused through the tubule lumen. A similar degree of red shift was observed for the intracellular carboxyfluorescein absorbance spectrum by J. A. Thomas et al. (1979). This red shift of the in vivo peak cannot be attributed to high $[Me_2CF]_i$, inasmuch as we failed to observe any in vitro red shift, even at dye concentrations as high as 10 mM. Thus, the red shift of the peak absorbance, along with the aforementioned independence of $A(peak)/A(470)$ on $[Me_2CF]$, indicates that the spectral characteristics of the dye are not the same in the cell as in the cuvette.

When the $A(511)/A(470)$ values of Fig. 8*B*, in addition to those of two similar experiments, are plotted as a function of nominal pH_i, the result is the pH titration curve of Fig. 10. For comparison, the in vitro pH titration curve at an $[Me_2CF]$ of 10 μM (Fig. 2, inset) is replotted in this figure. The curves drawn through the in vitro and in vivo data are the result of nonlinear least-squares

curve fits to a standard pH titration curve (see Tables II and III for fitting parameters). Although the upper and lower asymptotes of the two curves are very similar, the calculated pK_a value for the in vivo curve (7.35 ± 0.03) is 0.44 greater than for the in vitro curve (i.e., 6.90 ± 0.01). Even if the comparison

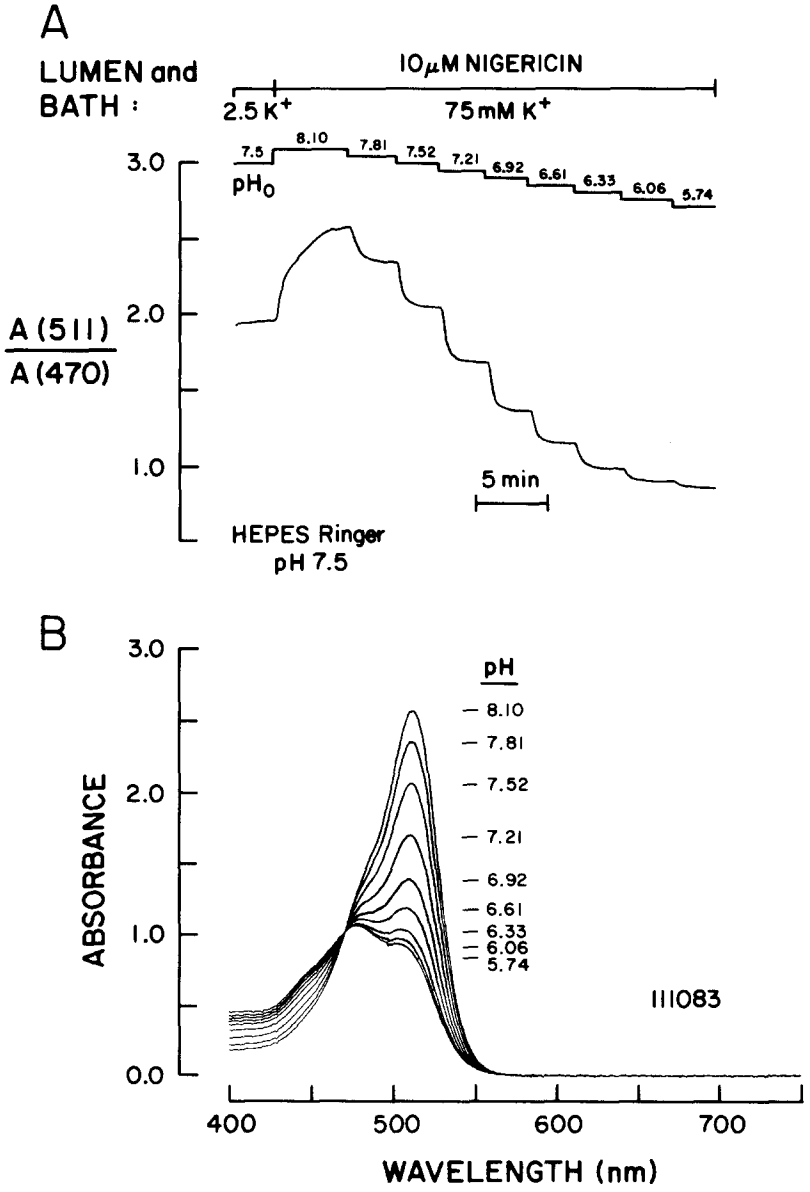

FIGURE 8. Calibration of intracellular dye. (*A*) Time course of $A(511)/A(470)$ while pH_i was varied. At the indicated time, luminal and basolateral solutions were changed from solution 1 to solution 5 (adjusted to pH 8.10). (*B*) Absorbance spectra obtained during periods of stable $A(511)/A(470)$ in the experiment of *A*.

between in vivo and in vitro titration curves are made at approximately equal dye concentrations, a sizable discrepancy persists. As shown in Table II, the in vitro pK_a at 3 mM Me_2CF is 7.05, still 0.30 lower than the in vivo value at a comparable dye concentration. One might object that the difference between intra- and extracellular pK_a values is a result of the procedure we used for cleansing total absorbance spectra for the absorbance caused by the tubule cells alone. However, if the second step of the procedure (the correction of Fig. 5, *E* and *F*) is omitted, the calculated pK_a value falls by only 0.03. Because this discrepancy between the in vivo and in vitro titration curves must be regarded

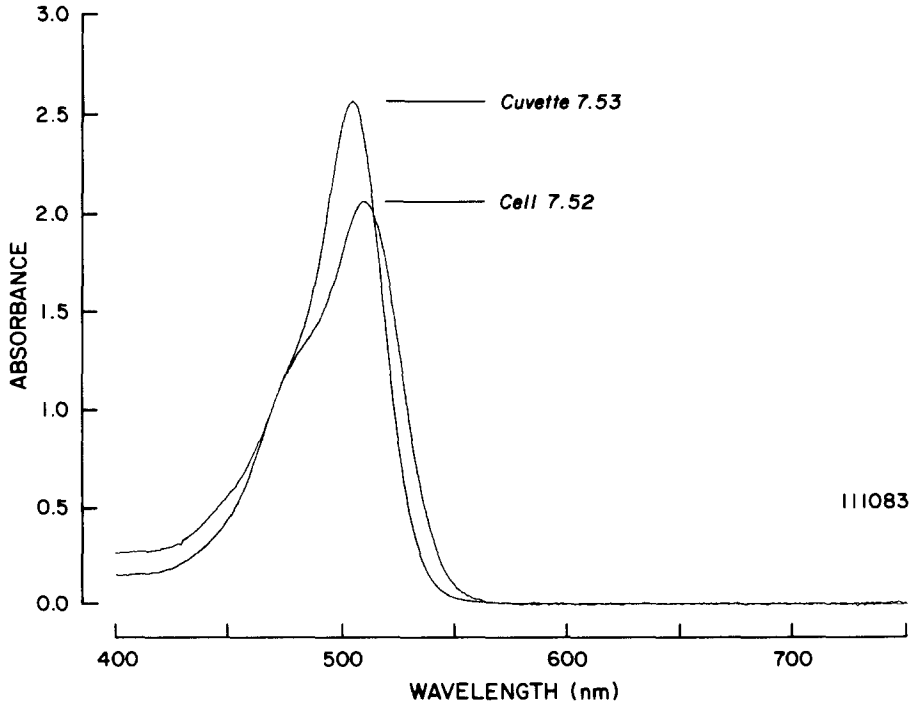

FIGURE 9. Comparison of in vitro and in vivo absorbance spectra at pH ~7.5. The cuvette spectrum was obtained from the experiment of Fig. 2, and the cell spectrum was obtained from the experiment of Fig. 8*B*.

as real, our initial approach of calculating pH_i from the in vitro curve is invalid. pH_i can only be calculated from an in vivo titration curve. For each of the three experiments in which a complete titration curve was obtained (see open symbols in Fig. 10), we calculated the initial pH_i from the tubule's own in vivo titration curve. The average, initial pH_i was 7.44 ± 0.09, which is not significantly different from the value of 7.43 ± 0.02 (n = 49), previously determined with pH-sensitive microelectrodes (Boron and Boulpaep, 1983*a*).

The intracellular data of Fig. 10 represent the results for the only three tubules for which a complete (i.e., over a broad pH_i range) calibration was obtained. We

have also obtained less extensive calibration data on 25 other tubules, pooled these data with those from the three complete experiments of Fig. 10, and analyzed these data pooled from 28 experiments (see Table III). The fitted pK (7.30 ± 0.04) was 0.05 lower than that derived for the data of the three complete experiments, and there was also a small difference in the value of the upper asymptote. The existence of these two similar but different calibration curves raises the issue of which, if either, is correct for all tubules in a large population. We suspect that the true dye calibration curve is somewhat different for each tubule. Thus, the best approach for calculating pH_i from dye data is to employ

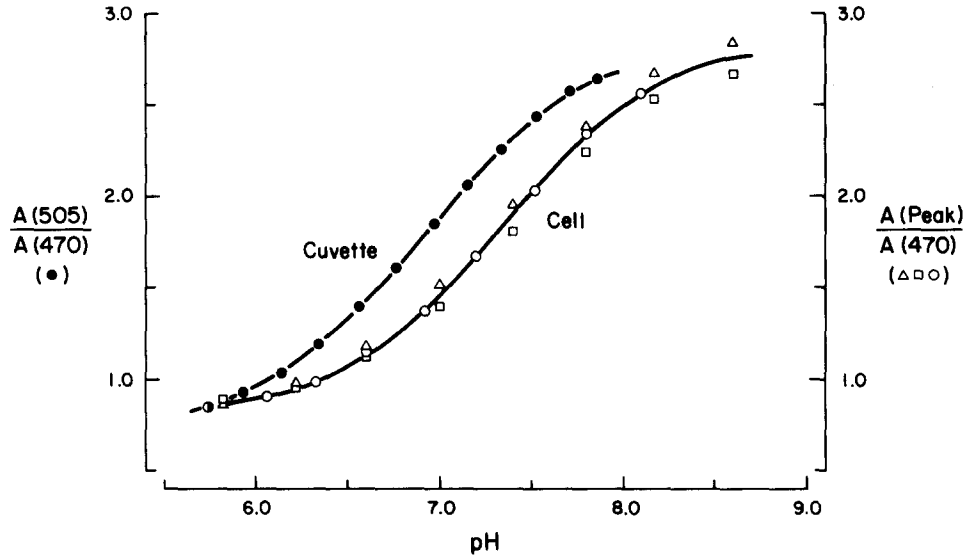

FIGURE 10. In vitro and in vivo dye calibration curves. The curve labeled "Cuvette" is replotted from the inset of Fig. 2. Its curve-fit parameters are those for 10 μM in Table II. The curve labeled "Cell" is the result of a nonlinear least-squares fit of the combined data from Fig. 8 and two similar experiments, all performed with the same solutions and over the course of 2 d. Its curve-fit parameters are those for the three pooled tubules in Table III. The wavelengths of peak dye absorbance in the three in vivo experiments were 511 (Fig. 8), 510, and 509 nm.

the dye calibration curve specific for each tubule, as was done for the three complete experiments above. If a complete curve does not exist for a tubule, the next best approach is to apply a calibration curve derived from the whole population (i.e., the pooled data). Using this approach, we calculated that the mean initial pH_i of the 28 tubules in the pooled group was 7.49 ± 0.03. This is significantly different statistically ($P < 0.005$) from the previously obtained microelectrode value of 7.43 ± 0.02 (Boron and Boulpaep, 1983*a*).

COMPARISON OF PH-SENSITIVE MICROELECTRODE AND DYE The preceding experiments suggest that an in vivo dye calibration, obtained for individual tubules or the whole population, yields an estimate of steady state pH_i that is

TABLE III

*Summary of Intracellular pH Titration Data for Me_2CF**

Sample	n	pK_a	Lower asymptote	Upper asymptote
(1) Tubule 111083	9	7.35±0.01	0.81±0.01	2.86±0.02
(2) Tubule 111183A	8	7.32±0.01	0.82±0.01	2.93±0.01
(3) Tubule 111183B	8	7.38±0.01	0.83±0.01	2.79±0.01
(4) 3 pooled tubules	25	7.35±0.03	0.82±0.02	2.86±0.03
(5) 28 pooled tubules	105	7.30±0.04	0.81±0.04	2.91±0.04

* Absorbance ratio data were fitted to a standard titration curve by a nonlinear least-squares method. Fitted values are listed ± standard deviation. n is the number points fitted. The "3 pooled tubules" are those listed in rows 1–3.

very similar (though not necessarily identical) to the value previously obtained with pH-sensitive microelectrodes. In six tubules, we were able to obtain an initial dye absorbance ratio, nigericin calibration data bracketing this initial ratio, and a simultaneous microelectrode measurement of the initial pH_i. The dye-derived pH_i values were calculated by linearly interpolating between the nigericin

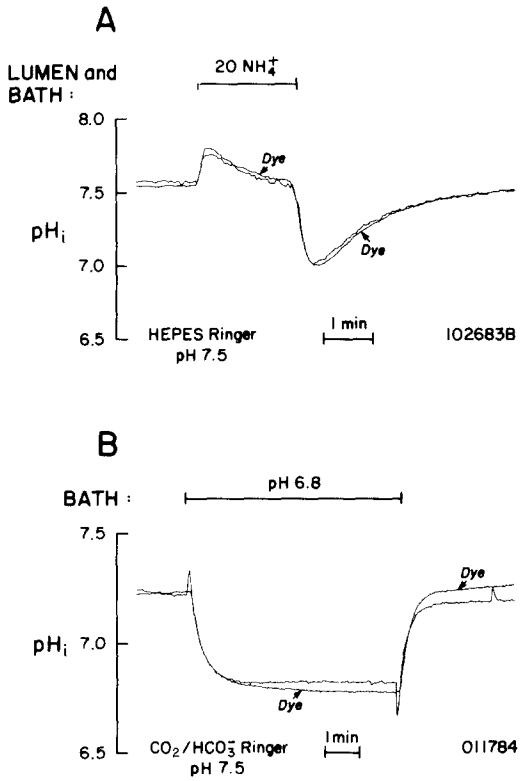

FIGURE 11. Simultaneous comparison of dye- and electrode-derived pH_i. (*A*) pH_i recovery from an NH_4^+-induced acid load in HEPES Ringer (solutions 1 and 2). The pH of the electrode tracing (unlabeled) was raised by 0.10. (*B*) pH_i response to basolateral acidification in HCO_3^- Ringer (solutions 6 and 7). The pH of the electrode tracing (unlabeled) was not offset.

data. The mean dye-derived pH_i was 7.50 ± 0.05 and the mean electrode-derived pH_i was 7.39 ± 0.06. The difference is statistically significant ($P \cong 0.03$, paired t test). Taken together with the data of the previous section, this result suggests that our approach for calculating a dye-derived pH_i yields values that slightly exceed those obtained with microelectrodes, perhaps by 0.1 pH unit.

In order to determine whether the dye can accurately follow rapid pH_i transients, we perturbed pH_i while simultaneously monitoring this parameter with the dye and a pH-sensitive microlectrode. Fig. 11 *A* illustrates an experiment in which tubule cells were briefly exposed to 20 mM NH_4^+ (see the discussion of Fig. 6*A* for a description of the pH_i changes). The baseline of the electrode-derived pH_i was raised by 0.1 to match the initial dye-derived pH_i. The pH_i changes measured by the dye are nearly identical to those recorded by the microelectrode. Qualitatively similar results were obtained in nine additional experiments. Fig. 11 *B* illustrates the results from one of three analogous experiments in which pH_i was altered by lowering $[HCO_3^-]_b$ from 10 to 2 mM (see the discussion of Fig. 6*B* for a description of pH_i changes). Once again, the time courses of the pH_i changes recorded by the two methods were very similar.

DISCUSSION

General

Our results indicate that the intracellular absorbance spectrum of Me_2CF can be used to measure steady state pH_i, and to follow rapid pH_i changes. The reliability of the method, however, depends critically on the dye calibration. Our data indicate that it is essential that the dye be calibrated inside the cell. Furthermore, it appears necessary to take into account tubule-to-tubule variability when calibrating the dye. Evidence for this variability includes: (*a*) the scatter among the "cell" absorbance ratios at high pH values for the three tubules of Fig. 10, (*b*) a similar scatter for the pooled data from 28 tubules (not shown), and (*c*) the differences among the fitted parameters for the extensive calibrations on three tubules and for the pooled calibration data on 28 tubules (see Table III). Tubule-to-tubule variations in the dye calibration are large enough that optimal results are obtained only when the dye is individually calibrated for each tubule. This, however, is impractical for most physiological experiments. We have found that when individual calibrations cannot be performed, the best agreement between dye- and microelectrode-derived pH_i values is obtained when a pooled dye calibration curve is employed, rather than a calibration curve for any particular tubule.

We have attempted to assess the accuracy of dye-derived pH_i values in three ways. (*a*) Extensive dye calibration curves were available for three individual tubules. The initial absorbance ratios for these tubules corresponded to a mean pH_i value (7.44 ± 0.03) that was very close to the mean microelectrode-derived value (7.43 ± 0.02) previously reported (Boron and Boulpaep, 1983*a*). (*b*) In six experiments, we were able to obtain microelectrode measurements of pH_i and, simultaneously, dye calibrations that bracketed the initial absorbance ratios. We found that the mean dye-derived pH_i (7.50 ± 0.05) was 0.11 higher than the microelectrode-derived value (7.39 ± 0.006). (*c*) Finally, in 28 experiments, we

obtained an initial absorbance ratio and some dye calibration data. These calibration data were combined to produce a pooled dye calibration curve, and this curve was used to convert initial dye absorbance ratios to initial dye-derived pH_i values for these 28 tubules. The mean dye-derived pH_i was 7.49 ± 0.03, 0.06 higher than the microelectrode-derived pH_i (7.43) previously obtained (Boron and Boulpaep, 1983*a*). Assuming that the microelectrode-derived pH_i is correct, our data indicate that our optical approach yields a pH_i value that is accurate to within ~0.1. If anything, the optical method errs on the alkaline side. We cannot determine from our data to what degree the slight inaccuracy of our dye-derived pH_i values is due to our optical apparatus, the intracellular behavior of the dye, or the nigericin calibration procedure. In any event, the accuracy of the dye method is more than sufficient for most physiological experiments.

One advantage of using Me_2CF is that, because its pK_a is in the physiologic range, it has a high sensitivity for measuring both increases and decreases of pH_i. In addition, the cells of the salamander proximal tubule are easily loaded with the dye, and maintain a high dye concentration long enough to permit one to perform useful experiments. This is in contrast to carboxyfluorescein, which we have found to be easily incorporated into the cells, but to be lost so rapidly as to preclude the execution of typical experiments. A potential limitation of using the absorbance spectrum to determine pH_i is that this method requires high intracellular concentrations of the dye. We estimate that $[Me_2CF]_i$ was 2–4 mM in most of our experiments. The buffering power of 4 mM dye at its pK would be ~2.3 mM, a small fraction of the 36-mM intrinsic or non-CO_2 buffering power of salamander proximal tubules (Boron and Boulpaep, 1983*a*). Furthermore, the dye does not appear to be toxic at the concentrations we used. Thus, our approach of calculating pH_i from the absorbance spectrum of Me_2CF promises to be of value for studying pH_i in cells in which the use of pH-sensitive microelectrodes is impractical. Indeed, we have successfully applied this technique to the proximal (Chaillet and Boron, 1984*a*) and cortical collecting tubules (Chaillet et al., 1985) of the rabbit, and to single cultured cells of the pig kidney cell line LLC-PK_1 (Chaillet et al., 1985).

Uncertainties in Calibrating Intracellular Me_2CF

DOES NIGERICIN EQUILIBRATE pH_i AND pH_o? Our intracellular calibration procedure requires that nigericin make the cytoplasmic pH (i.e., pH_i) equal to pH_o. Ideally, this would be verified with microelectrodes. Unfortunately, direct verification was precluded because nigericin significantly alters the properties of the liquid membrane pH-sensitive microelectrodes in an unpredictable manner. Furthermore, the combination of nigericin and high K^+ would supposedly reduce both the voltage and the pH differences across the membrane to near-zero values. Because of this, the only way to verify that the pH and voltage microelectrodes were inside the cells would be to monitor an apparent recovery of pH_i and V_m upon removal of the nigericin and return of $[K^+]_o$ to 2.5 mM. As noted in the Results, we were able to accomplish the latter in four experiments, and thereby verify that the nigericin/high-K^+ combination drives V_m to near-zero values. Although we cannot verify the nigericin equilibration procedure directly, we can model the effects of nigericin and compare the predictions with our data.

Assume that nigericin exchanges K^+ for H^+, and that at equilibrium

$$\frac{[K^+]_i}{[K^+]_o} = \frac{[H^+]_i}{[H^+]_o} = \frac{10^{-pH_i}}{10^{-pH_o}},$$

where activities are understood in place of concentrations, and the subscripts i and o refer to intra- and extracellular values, respectively. If the initial pH_o (pH_o^i) is now increased by the amount ΔpH_o, H^+ will leave the cell in exchange for K^+. The initial $[K^+]_i$ ($[K^+]_i^i$) will increase by the amount x, to reach the final value of $[K^+]_i^f$. Simultaneously, the initial pH_i (pH_i^i) will increase by x/β (where β is the total intracellular buffering power), to reach the final value of pH_i^f. When the new equilibrium is reached,

$$\frac{[K^+]_i^f}{[K^+]_o^f} = \frac{[K^+]_i^i + x}{[K^+]_o^i} = \frac{10^{-(pH_i^i + x/\beta)}}{10^{-(pH_o^i + \Delta pH_o)}} = \frac{10^{-pH_i^f}}{10^{-pH_o^f}}.$$

We can solve for x numerically, and thus determine $[K^+]_i^f$ and pH_i^f. In the simplest case, pH_i^i and pH_o^i values are equal, as are $[K^+]_i^i$ and $[K^+]_o^i$. Even in this example, however, the model predicts that a change in pH_o must result in an equilibrium in which $pH_i^f \neq pH_o^f$ and $[K^+]_i^f \neq [K^+]_o^f$. The discrepancy between pH_i^f and pH_o^f increases as the magnitude of the pH_o change increases. This line of reasoning suggests that the in vivo pH titration curve of Fig. 10 is in error, inasmuch as we had assumed that pH_i always equals pH_o. Consider as an example the calibration experiment of Fig. 8, in which the titration curve (indicated by the open circles in Fig. 10) has a calculated pK_a of 7.35 (see line 1 of Table IV). Assume that $pH_i^i = pH_o^i = 7.35$, and that $[K^+]_i^i = [K^+]_o^i = 75$ mM. We used this model to calculate revised pH_i values during the titration, fitted these revised data to a standard pH titration curve (see line 2 of Table IV), and plotted the revised calibration curve (along with the original titration curve) in the upper portion of Fig. 12. The pK_a of this revised titration curve is 7.38 ± 0.02, compared with the original pK_a of 7.35 ± 0.01. The asymptotes of the revised curve were also modestly altered.

The above discussion assumed that $[K^+]_i^i = [K^+]_o^i = 75$ mM at the initial pH_i of 7.35. However, if $[K^+]_i^i$ were only 55 mM (Fig. 12, middle), the revised pK_a would increase from 7.35 ± 0.01 to 7.53 ± 0.03 (see line 3 of Table IV). Conversely, if $[K^+]_i^i$ were 95 mM (Fig. 12, bottom), the revised pK_a would fall to 7.28 ± 0.02 (see line 4 of Table IV). In both cases, the shifts in the pK_a values would be accompanied by correspondingly large changes in the values of the asymptotes.

Although the model predicts that the revised titration curves are different from the original one, the predicted pH_i errors are large only at extreme pH_i values. For a $[K^+]_i^i$ of 75 mM, errors in the estimated pH_i^f of ~0.2 would occur at apparent pH_i^f values of 6.2 and 8.2. If $[K^+]_i^i$ were 55 mM, the error would be negligible at the apparent pH_i^f of 8.2, but would be ~0.5 at the apparent pH_i^f of 6.2. Finally, for a $[K^+]_i^i$ of 95 mM, the error would be only ~0.1 at this apparent pH_i^f of 6.2, but ~0.3 at the apparent pH_i^f of 8.2. The magnitude of even these larger errors would not preclude using the dye for semiquantitative measurements. However, three lines of evidence suggest that the cumulative errors in

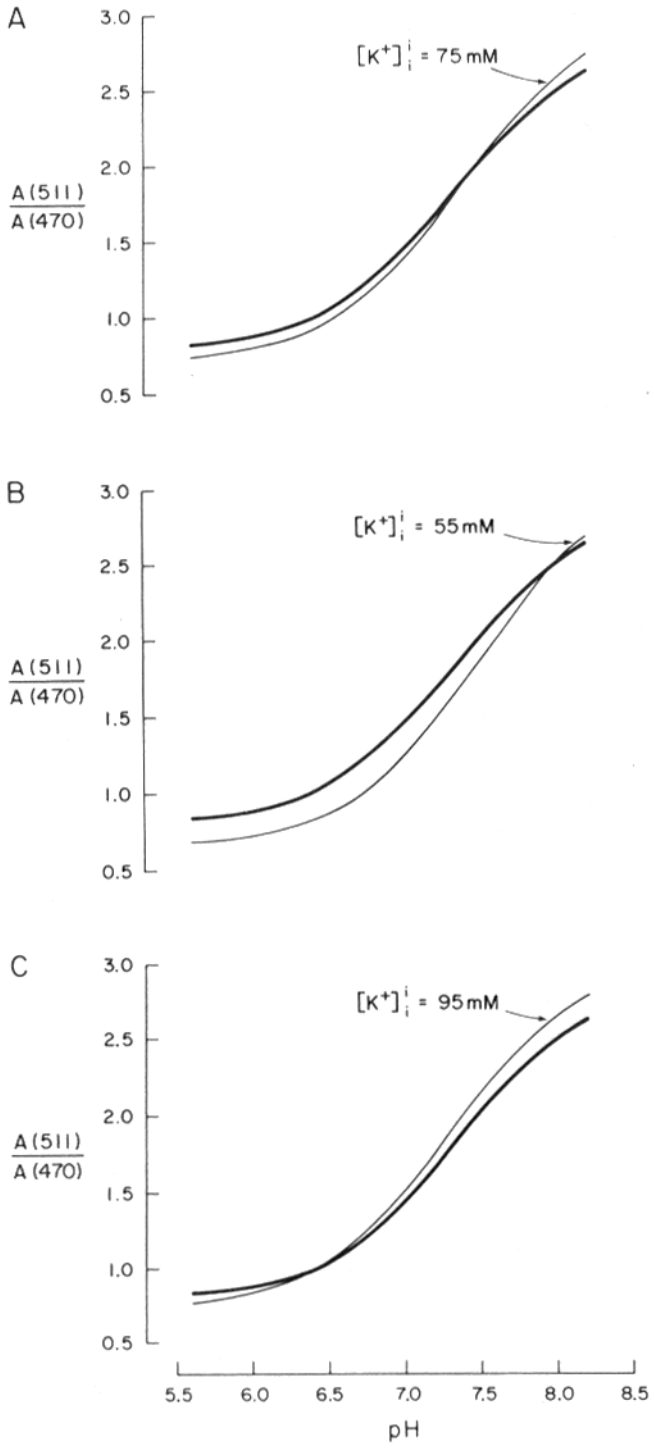
A
B
C
$[K^+]_i^i$ = 75 mM
$[K^+]_i^i$ = 55 mM
$[K^+]_i^i$ = 95 mM
A(511)/A(470)
3.0
2.5
2.0
1.5
1.0
0.5
5.5
6.0
6.5
7.0
7.5
8.0
8.5
pH

FIGURE 12.

the nigericin technique are in fact small enough to permit quantitative measurements of pH_i.

The first line of evidence is that, in high-K^+ nigericin solutions, the cell voltage (V_m) approaches zero. In the above example, for which $[K^+]_i^f$ is assumed to be 55 mM, the pH_i^f error of ~0.5 requires $[K^+]_o^f/[K^+]_i^f$ to be 75 mM/17 mM. If the cell membrane were perfectly K^+ selective, this ratio would produce a V_m of +38 mV. We found that application of nigericin at $[K^+]_o$ = 75 mM caused V_m to approach 0 mV at pH_o values between ~6 and ~8. This suggests that the K^+ gradient, and therefore the pH gradient, is small.

The second line of evidence is that changing $[K^+]_o$ has only a minor effect on $A(peak)/A(470)$. As noted in the Results, we found that raising or lowering $[K^+]_o$ by 10 mM, at a pH_o of either 8.0 or 6.8, causes apparent shifts in the dye-derived pH_i of 0.04 to 0.06. Thus, even if the chosen $[K^+]_o$ were in error by as much as 10 mM, the effect on the intracellular dye calibration curve would be minor.

TABLE IV

*Summary of pH Titration Data for Fig. 12**

Sample	Assumed $[K^+]_i^f$	pK_a	Lower asymptote	Upper asymptote
	mM			
(1) Tubule 111083	—	7.35±0.01	0.81±0.01	2.86±0.02
(2) Nigericin model	75	7.38±0.02	0.71±0.01	3.04±0.03
(3) Nigericin model	55	7.53±0.03	0.66±0.02	3.11±0.04
(4) Nigericin model	95	7.29±0.02	0.74±0.01	3.02±0.02

* Absorbance ratio data were fitted to a standard titration curve by a nonlinear least-squares method. Fitted values are listed ± standard deviation.

The final line of evidence suggesting that the nigericin method approximately equalizes pH_i and pH_o is the agreement between dye- and electrode-derived pH_i measurements. Our observation that the steady state dye-derived pH_i is within ~0.1 of the microelectrode-derived pH_i suggests that, at normal pH values, nigericin does indeed approximately equate pH_i and pH_o. In addition, the close agreement between the dye and microelectrode during acidic and alkaline

FIGURE 12. (*opposite*) Predicted modifications of in vivo pH calibration curve. (*A*) Assumed initial $[K^+]_i$ = 75 mM at pH_i = 7.35. The bold curve is a nonlinear, least-squares fit to the data of Fig. 8. Its curve-fit parameters are given in line 1 of Table IV. The data for the labeled curve were derived from those of Fig. 8, using the nigericin model described in the text. These data were fitted by a nonlinear least-squares method, the curve-fit parameters for which are given in line 2 of Table IV. (*B*) Assumed initial $[K^+]_i$ = 55 mM at pH_i = 7.35. The curve-fit parameters for the model curve are given in line 3 of Table IV. (*C*) Assumed initial $[K^+]_i$ = 95 mM at pH_i = 7.38. The curve-fit parameters for the model curve are given in line 4 of Table IV.

transients (Fig. 11) indicates that the method is valid over the range of pH_i values likely to be encountered experimentally.

DOES IT MATTER IF THE DYE IS COMPARTMENTALIZED WITHIN THE CELL? We have yet to consider the possibility that the dye may be compartmentalized within the cell. During rapid changes in pH_i, there are large absorbance changes that have the same time course as the pH_i changes measured with a microelectrode (Fig. 11, *A* and *B*). The absorbance changes are so large as to require that nearly all of the dye respond almost instantaneously to the pH changes. Thus, if a large portion of the dye is in an intracellular subcompartment, then the pH of the subcompartment must rapidly follow the pH of the cytoplasm. The dye must, therefore, be in the cytoplasm monitoring pH_i directly and/or in a subcompartment monitoring pH_i indirectly. In any case, the simultaneous microelectrode-dye comparison indicates that the properly calibrated dye monitors pH_i with reasonable accuracy.

IS THE DYE METABOLIZED OR BOUND TO INTRACELLULAR COMPONENTS? Three characteristics of the intracellular dye's absorbance spectrum are consistent with metabolism or binding of the dye. (*a*) Compared with the in vitro dye, intracellular dye has an absorbance peak that is red-shifted 3–6 nm, and an isosbestic wavelength that is red-shifted by 1–6 nm. Thus, it appears that the entire absorbance spectrum, above wavelengths of 470 nm, is red-shifted. (*b*) The pK_a of intracellular Me_2CF is a substantially higher than that of the in vitro dye. (*c*) The intracellular absorbance spectrum is insensitive to changes in dye concentration in the 1–4-mM range. The progressive fall of $A(505)/A(470)$ with increasing $[Me_2CF]$ in vitro is probably due to dye-dye interactions. The absence of this effect in vivo would be expected if dye binding or metabolism prevented such dye-dye interactions.

Metabolism or binding of the dye are not the only factors that could affect the absorbance spectrum or pH sensitivity of Me_2CF. It is well known (see Walker and Richards, 1959) that both light scattering and the inhomogeneous distribution of dye modify absorbance. However, errors secondary to light scattering should have been minimized in our experiments, inasmuch as we corrected our spectra for changes in intrinsic absorbance. Another potential complication is that the dye's pK_a is likely to be influenced by ionic composition and ionic strength, both of which could vary in different regions of the cell. Although the effects of these multiple factors on dye behavior probably invalidate calculating pH_i from in vitro calibration spectra, they by no means preclude the use of the dye's absorbance spectrum for measuring pH_i, provided an intracellular calibration is obtained. In fact, the shift of the pK_a and the absence of the dye concentration effect are advantageous for the accurate measurement of pH_i and pH_i changes.

We thank Drs. E. L. Boulpaep, L. H. Cohen, and D. G. Warnock for their helpful comments on an earlier draft of this manuscript. We are deeply indebted to Mr. Andrey Yeatts for interfacing the photodiode array to the computer, and for writing many of the computer programs. We also thank Mr. Roger Kankal for manufacturing the microelectrodes.

This research was supported by National Institutes of Health grant R01 AM30344. J.R.C. was supported by National Institutes of Health predoctoral training grant GM07527 and by an

American Heart Association (Connecticut affiliate) postdoctoral training fellowship (11-104-834). W.F.B. was a Searle Scholar during the execution of the research, and was supported for part by the time by a Research Career Development Award (K01 AM01022).

Original version received 6 August 1984 and accepted version received 30 July 1985.

REFERENCES

Ammann, D., F. Lanter, R. A. Steiner, P. Schulthess, Y. Shijo, and W. Simon. 1981. Neutral carrier based hydrogen ion selective microelectrode for extra- and intracellular studies. *Anal. Chem.* 53:2267–2269.

Babcock, D. F. 1983. Examination of the intracellular ionic environment and of ionophore action by null point measurements employing the fluorescein chromophore. *J. Biol. Chem.* 258:6380–6389.

Balaban, R. S. 1982. Nuclear magnetic resonance studies of epithelial metabolism and function. *Fed. Proc.* 41:42–47.

Baxendale, L. M., and W. M. Armstrong. 1983. Doubled-barreled liquid membrane microelectrodes for measuring intracellular pH. *J. Gen. Physiol.* 87:17*a*. (Abstr.)

Bichara, M., M. Paillard, F. Leviel, and J.-P. Gardin. 1980. Hydrogen transport in rabbit kidney proximal tubules—Na:H exchange. *Am. J. Physiol.* 238:F445–F451.

Boron, W. F., and E. L. Boulpaep. 1983*a*. Intracellular pH regulation in the renal proximal tubule of the salamander: Na-H exchange. *J. Gen. Physiol.* 81:29–52.

Boron, W. F., and E. L. Boulpaep. 1983*b*. Intracellular pH regulation in the renal proximal tubule of the salamander: basolateral HCO_3^- transport. *J. Gen. Physiol.* 81:53–94.

Boron, W. F., and P. De Weer. 1976. Intracellular pH transients in squid giant axons caused by CO_2, NH_3, and metabolic inhibitors. *J. Gen. Physiol.* 67:91–112.

Burg, M., J. Grantham, M. Abramow, and J. Orloff. 1966. Preparation and study of fragments of single rabbit nephrons. *Am. J. Physiol.* 210:1293–1298.

Chaillet, J. R., and W. F. Boron. 1984*a*. Intracellular pH regulation in rabbit proximal tubules studied with a pH-sensitive dye. *Kidney Int.* 25:273. (Abstr.)

Chaillet, J. R., and W. F. Boron. 1984*b*. Basolateral Na-H exchange in the rabbit cortical collecting tubule. *Fed. Proc.* 43:1089. (Abstr.)

Chaillet, J. R., Lopes, A. G., and W. F. Boron. 1985. Basolateral Na-H exchange in the rabbit cortical collecting tubule. *J. Gen. Physiol.* 86:795–812.

Duffey, M. E., and G. Bebernitz. 1983. Intracellular chloride and hydrogen activities in rabbit colon. *Fed. Proc.* 42:1353. (Abstr.)

Eaton, D. C., K. L. Hamilton, and K. E. Johnson. 1984. Intracellular acidosis blocks the basolateral Na-K pump in rabbit urinary bladder. *Am. J. Physiol.* 247:F946–F954.

Kleinman, J. G., W. W. Brown, R. A. Ware, and J. H. Schwartz. 1980. Cell pH and acid transport in renal cortical tissue. *Am. J. Physiol.* 239:F440–F444.

Khuri, R. N., J. J. Hajjar, and S. K. Agulian. 1972. Intracellular potassium in cells of the proximal tubule of *Necturus maculosus*. *Pflügers Arch. Eur. J. Physiol.* 388:73–80.

Kubota, T., B. Biagi, and G. Giebisch. 1980. Intracellular K^+ activity measurements in single proximal tubules of *Necturus* kidney. *Curr. Top. Membr. Transp.* 13:63–72.

Moolenaar, W. H., R. Y. Tsien, P. T. vander Saag, and S. W. de Laat. 1983. Na^+/H^+ exchange and cytoplasmic pH in the action of growth factors in human fibroblasts. *Nature (Lond.).* 304:645–648.

Pressman, B. C. 1976. Biological applications of ionophores. *Annu. Rev. Biochem.* 45:501–530.

Rink, T. J., R. Y. Tsien, and T. Pozzan. 1982. Cytoplasmic pH and free Mg^{2+} in lymphocytes. *J. Cell Biol.* 95:189–196.

Rothenberg, P., L. Glaser, P. Schlesinger, and D. Cassel. 1983. Activation of Na^+/H^+ exchange by epidermal growth factor elevates intracellular pH in A431 cells. *J. Biol. Chem.* 258:12644–12653.

Rotman, B., and B. Papermaster. 1966. Membrane properties of living mammalian cells as studied by enzymatic hydrolysis of fluorogenic esters. *Proc. Natl. Acad. Sci. USA.* 55:134–141.

Sackin, H., and E. L. Boulpaep. 1981. Isolated perfused salamander proximal tubule. II. Monovalent ion replacement and rheogenic transport. *Am. J. Physiol.* 241:F540–F555.

Sasaki, S., Y. Iino, T. Shiigai, and J. Takeuchi. 1984. Intracellular pH of isolated perfused rabbit proximal tubule: effects of luminal Na and Cl. *Kidney Int.* 25:282. (Abstr.)

Sehr, P. A., P. J. Bore, J. Papatheofanis, and G. K. Radda. 1979. Non-destructive measurement of metabolites and tissue pH in the kidney by ^{31}P nmr. *Br. J. Exp. Pathol.* 60:632–639.

Struyvenberg, A., R. B. Morrison, and A. S. Relman. 1968. Acid-base behavior of separated canine renal tubule cells. *Am. J. Physiol.* 214:1155–1162.

Talmi, Y., and R. W. Simpson. 1980. Self-scanned photodiode array: a multichannel spectrometric detector. *Appl. Opt.* 19:1401–1414.

Thomas, J. A., R. N. Buchsbaum, A. Zimniak, and E. Racker. 1979. Intracellular pH measurements in Ehrlich ascites tumor cells utilizing spectroscopic probes generated in situ. *Biochemistry.* 81:2210–2218.

Thomas, R. C. 1974. Intracellular pH of snail neurones measured with a new pH-sensitive glass micro-electrode. *J. Physiol. (Lond.).* 238:159–180.

Tsien, R. Y. 1981. A non-disruptive technique for loading calcium buffers and indicators into cells. *Nature (Lond.).* 290:527–528.

Vigne, P., C. Frelin, and M. Lazdunski. 1982. The amiloride-sensitive Na^+/H^+ exchange system in skeletal muscle cells in culture. *J. Biol. Chem.* 257:9394–9400.

Walker, P. M. B., and B. M. Richards. 1959. Quantitative microscopical techniques for single cells. *In* The Cell. J. Brachet and A. E. Mirsky, editors. Academic Press, Inc., New York. 1:91–138.